

On a convergent DSA preconditioned source iteration for a DGFEM method for radiative transfer

Olena Palii, Matthias Schlottbom*

Department of Applied Mathematics, University of Twente, P.O. Box 217, 7500 AE Enschede, The Netherlands



ARTICLE INFO

Article history:

Received 17 July 2019
Received in revised form 10 January 2020
Accepted 1 February 2020
Available online 22 February 2020

Keywords:

Radiative transfer
Discontinuous angular approximation
Discrete ordinates method
Diffusion synthetic acceleration
Convergence rates

ABSTRACT

We consider the numerical approximation of the radiative transfer equation using discontinuous angular and continuous spatial approximations for the even parts of the solution. The even-parity equations are solved using a diffusion synthetic accelerated source iteration. We provide a convergence analysis for the infinite-dimensional iteration as well as for its discretized counterpart. The diffusion correction is computed by a subspace correction, which leads to a convergence behavior that is robust with respect to the discretization. The proven theoretical contraction rate deteriorates for scattering dominated problems. We show numerically that the preconditioned iteration is in practice robust in the diffusion limit. Moreover, computations for the lattice problem indicate that the presented discretization does not suffer from the ray effect. The theoretical methodology is presented for plane-parallel geometries with isotropic scattering, but the approach and proofs generalize to multi-dimensional problems and more general scattering operators verbatim.

© 2020 The Authors. Published by Elsevier Ltd. This is an open access article under the CC BY license (<http://creativecommons.org/licenses/by/4.0/>).

1. Introduction

We consider the numerical solution of the radiative transfer equation in plane parallel geometry

$$\mu \partial_z \phi(z, \mu) + \sigma_t(z) \phi(z, \mu) = \frac{\sigma_s(z)}{2} \int_{-1}^1 \phi(z, \mu') d\mu' + q(z, \mu), \quad (1)$$

where $0 < z < Z$ and $-1 < \mu < 1$, and Z denotes the thickness of the slab and μ is the cosine of the polar angle of a unit vector. The function $\phi(z, \mu)$ models the equilibrium distribution of some quantity, like neutrons or photons [1,2]. The basic physical principles embodied in (1) are transport, which is modeled by the differential operator $\mu \partial_z$, absorption with rate $\sigma_a = \sigma_t - \sigma_s$ and scattering with rate σ_s . Internal sources are described by the function q . In this work we close the radiative transfer equation using inflow boundary conditions

$$\phi(0, \mu) = g^0(\mu) \quad \mu > 0, \quad \text{and} \quad \phi(Z, \mu) = g^Z(\mu) \quad \mu < 0. \quad (2)$$

Such transport problems arise when the full three-dimensional model posed on $\mathbb{R}^2 \times (0, Z) \times \mathbb{S}^2$ obeys certain symmetries [2]. It has been studied in many instance due to simpler structure compared to three dimensional problems without symmetries; the methodology presented here directly carries over to the general case, see also the numerical examples presented below.

* Corresponding author.

E-mail addresses: o.palii@utwente.nl (O. Palii), m.schlottbom@utwente.nl (M. Schlottbom).

Classical deterministic discretization strategies are based on a semidiscretization in μ . One class of such strategies are the P_N -approximations, which are spectral methods based on truncated spherical harmonics expansions [3,4], and we refer to [5–7] for variational discretization strategies using this approximation. The major advantage of P_N -approximations is that the scattering operator becomes diagonal. In addition, the matrix representation of the transport operator $\mu\partial_z$ is sparse. The main drawbacks of the P_N -method are that the variational incorporation of the inflow boundary condition introduces a dense coupling of the spherical harmonics expansion coefficients making standard P_N -approximations quite expensive to solve. We note, however, that a modified variational formulation of the P_N -equations has recently been derived that leads to sparse matrices [8]. In any case, the success of spectral approximation techniques depends on the smoothness of the solution. In general, the solution ϕ is not smooth for $\mu = 0$, which is related to the inflow boundary conditions (2). Hence, the P_N -approximations will in general not converge spectrally. Resolving the non-smoothness of ϕ should improve the approximation considerably, and this observation led to the developments of double P_N -methods [4] or half space moment methods [9,10], which are spectral methods on the intervals $\mu > 0$ and $\mu < 0$.

A second class of semidiscretizations are discrete ordinates methods that use a quadrature rule for the discretization of the μ -variable [2], with analysis provided in [11,12]. Such methods are closely related to discontinuous Galerkin (DG) methods, see, e.g., [13–18]. While allowing for local angular resolution, the main obstruction in the use of these methods is that the scattering operator leads to dense matrices, and a direct inversion of the resulting system is not possible in realistic applications. To overcome this issue, iterative solution techniques have been proposed. An often used iterative technique is Richardson iteration, i.e., the source iteration [19–21], but other Krylov space methods exist [22]. The key idea of the source iteration is to decouple scattering and transport, and to exploit that the transport part can be inverted efficiently. If $\sigma_s/\sigma_t \approx 1$, the convergence of these iterative methods is slow, and several preconditioning techniques have been proposed [16,19,20,22]. Among the most used and simple preconditioners is the diffusion synthetic acceleration method (DSA), in which a diffusion problem is solved in every iteration. This is well motivated by asymptotic analysis [23,24]. While Fourier analysis can be applied to special situations [19,20], the convergence analysis is mainly open for the general case, i.e., for non-constant coefficients or non-periodic boundary conditions. A further complication in using the DSA preconditioner is that the resulting iterative scheme might diverge if the discretization of the diffusion problem and the discrete ordinates system are not consistent [20].

For isotropic scattering, integral methods for the approximation of the angular average of the solution have been proposed recently [25]. The efficiency of the iterative solver of [25] deteriorates if scattering becomes dominant, and a diffusion-based preconditioner is employed to reduce the number of iterations. Extensions to anisotropic scattering can be found in [26].

The contribution of this paper is to develop discretizations that allow for local resolution of the non-smoothness of the solution, and which lead to discrete problems that can be solved efficiently by diffusion synthetic accelerated source iterations. Our approach builds upon an even-parity formulation of the radiative transfer equation derived from the mixed variational framework given in [7], where P_N -approximations have been treated in detail. We show that our DSA preconditioned source iteration converges already for the continuous problem. We present conforming hp -type approximation spaces for the discretization, and prove quasi-best approximation properties of the Galerkin approximation. In order to solve the resulting linear systems, we employ a DSA preconditioned Richardson iteration, which is just the infinite dimensional iteration projected to the approximation spaces. In particular the finite dimensional iteration is guaranteed to converge for any discretization. Moreover, the inversion of the transport problem can be parallelized straightforward. In numerical experiments, even when employing low-order approximations, we observe that the developed method does not suffer from the ray effect, which is typically observed for discrete ordinates methods [4,27].

The outline of the paper is as follows: In Section 2 we introduce basic notation and recall the relevant function spaces. In Section 3 we introduce the even-parity equation for (1), show its well-posedness, and formulate an infinite dimensional DSA preconditioned source iteration, for which we show convergence. The approximation spaces are described in Section 4 and well-posedness of the Galerkin problems as well as quasi-best approximation results are presented. In Section 5 we discuss the efficient iterative solution of the resulting linear systems and provide a convergence proof for the discrete DSA scheme. Section 6 presents supporting numerical examples for slab geometry and for multi-dimensional problems that show the good approximation properties of the proposed method as well as fast convergence of the iterative solver in multi-dimensional problems and in the diffusion limit. The paper ends with some conclusions in Section 7.

2. Function spaces and further preliminaries

Following [28] we denote by $L^2(\mathcal{D})$ with $\mathcal{D} = (0, Z) \times (-1, 1)$ the usual Hilbert space of square integrable functions with inner product

$$(\phi, \psi) = \int_{-1}^1 \int_0^Z \phi(z, \mu)\psi(z, \mu) dz d\mu$$

and induced norm $\|\phi\|_{L^2(\mathcal{D})} = (\phi, \phi)^{\frac{1}{2}}$. Furthermore, we define the Hilbert space

$$H_2^1(\mathcal{D}) = \{\phi \in L^2(\mathcal{D}) : \mu\partial_z\phi \in L^2(\mathcal{D})\}$$

of functions with square integrable weak derivatives with respect to the weighted differential operator $\mu \partial_z$ endowed with the corresponding graph norm.

In order to deal with boundary data, let us introduce the Hilbert space L^2_- that consists of measurable functions for which

$$\|\psi\|_{L^2_-}^2 = \int_0^1 |\psi(0, \mu)|^2 |\mu| d\mu + \int_{-1}^0 |\psi(Z, \mu)|^2 |\mu| d\mu$$

is finite, and we denote by $\langle \psi, \phi \rangle_{L^2_-}$ the corresponding inner product on L^2_- . Similarly, L^2_+ denotes the space of outflow data. We have the following trace lemma [28].

Lemma 2.1. *If $\phi \in H^1_2(\mathcal{D})$, then there exist traces $\phi|_{\Gamma_-} \in L^2_-$ and $\phi|_{\Gamma_+} \in L^2_+$ and*

$$\|\phi|_{\Gamma_{\pm}}\|_{L^2_{\pm}} \leq \frac{C}{\sqrt{1 - e^{-Z}}} \|\phi\|_{H^1_2(\mathcal{D})}$$

with a constant $C > 0$ independent of ϕ and Z .

As a consequence of the trace lemma and the density of smooth functions in $H^1_2(\mathcal{D})$ the following integration-by-parts formula is true [28]

$$(\mu \partial_z \phi, \psi) = -(\phi, \mu \partial_z \psi) + \langle \phi, \psi \rangle_{L^2_+} - \langle \phi, \psi \rangle_{L^2_-}. \tag{3}$$

Throughout the manuscript we make the following basic assumption:

(A1) $\sigma_s, \sigma_t \in L^\infty(0, Z)$ are non-negative and $\sigma_a = \sigma_t - \sigma_s \geq \gamma > 0$.

Assumption (A1) means that we consider absorbing media, which makes (1)–(2) well-posed [28].

Lemma 2.2. *Let assumption (A1) hold, and let $g \in L^2_-$ and $q \in L^2(\mathcal{D})$, then (1)–(2) has a unique solution $\phi \in H^1_2(\mathcal{D})$ that satisfies the a-priori bound*

$$\|\phi\|_{H^1_2(\mathcal{D})} \leq C(\|g\|_{L^2_-} + \|q\|_{L^2(\mathcal{D})}).$$

Assumption (A1) is not required to prove well-posedness for bounded geometries [29], or for slab problems with constant coefficients [30, Thm. 2.25].

Let $\mathcal{P} : L^2(\mathcal{D}) \rightarrow L^2(\mathcal{D})$ denote the L^2 -projection onto constants in μ , i.e.,

$$(\mathcal{P}\psi)(z, \mu) = \frac{1}{2} \int_{-1}^1 \psi(z, \mu') d\mu'.$$

Since $\sigma_t \in L^\infty(0, Z)$ is strictly positive, we can define the following norms on $L^2(\mathcal{D})$

$$\|\psi\|_{\sigma_t}^2 = (\sigma_t \psi, \psi) \quad \text{and} \quad \|\psi\|_{\frac{1}{\sigma_t}}^2 = \left(\frac{1}{\sigma_t} \psi, \psi\right). \tag{4}$$

2.1. Even-odd splitting

The even and odd parts of a function $\phi \in L^2(\mathcal{D})$, denoted by ϕ^+ and ϕ^- , respectively, are defined as

$$\phi^+(z, \mu) = \frac{1}{2}(\phi(z, \mu) + \phi(z, -\mu)), \quad \phi^-(z, \mu) = \frac{1}{2}(\phi(z, \mu) - \phi(z, -\mu)).$$

Even-odd decompositions are frequently used in transport theory [3,5]. Since, as functions of μ , even and odd function are orthogonal in $L^2(-1, 1)$, we can decompose $L^2(\mathcal{D})$ into orthogonal subspaces containing even and odd functions, respectively,

$$L^2(\mathcal{D}) = L^2(\mathcal{D})^+ \oplus L^2(\mathcal{D})^-.$$

Similarly, we will write $H^1_2(\mathcal{D})^\pm = H^1_2(\mathcal{D}) \cap L^2(\mathcal{D})^\pm$. As in [7], we observe that $\mu \partial_z \phi^\pm \in L^2(\mathcal{D})^\mp$ for any $\phi \in H^1_2(\mathcal{D})$, and $\mathcal{P}\phi^\pm \in L^2(\mathcal{D})^+$ for $\phi \in L^2(\mathcal{D})$. It turns out that the natural space for our formulation is

$$\mathbb{W} = H^1_2(\mathcal{D})^+ \oplus L^2(\mathcal{D})^-.$$

3. Weak formulation of the slab problem

3.1. Derivation

We follow the steps presented in [7] for multi-dimensional problems. The key idea is to rewrite the slab problem into a weak formulation for the even and odd parts of the solution. Multiplication of (1) with a test function $\psi \in \mathbb{W}^+$ and

using orthogonality of even and odd functions gives that

$$(\mu \partial_z \phi^-, \psi^+) + ((\sigma_t - \sigma_s \mathcal{P})\phi^+, \psi^+) = (q^+, \psi^+).$$

Integration-by-parts (3) applied to the first term on the left-hand side yields that

$$(\mu \partial_z \phi^-, \psi^+) = -\langle \phi^-, \mu \partial_z \psi^+ \rangle + \langle \phi^-, \psi^+ \rangle_{L^2_+} - \langle \phi^-, \psi^+ \rangle_{L^2_-}.$$

Due to symmetries, we have that $\langle \phi^-, \psi^+ \rangle_{L^2_+} = -\langle \phi^-, \psi^+ \rangle_{L^2_-}$. Using (2), we have that $\phi^- = \phi - \phi^+ = g - \phi^+$ on the inflow boundary, which leads to

$$(\mu \partial_z \phi^-, \psi^+) = -\langle \phi^-, \mu \partial_z \psi^+ \rangle + 2\langle \phi^+, \psi^+ \rangle_{L^2_-} - 2\langle g, \psi^+ \rangle_{L^2_-}.$$

Thus, for any $\psi^+ \in \mathbb{W}^+$, it holds that

$$2\langle \phi^+, \psi^+ \rangle_{L^2_-} - \langle \phi^-, \mu \partial_z \psi^+ \rangle + ((\sigma_t - \sigma_s \mathcal{P})\phi^+, \psi^+) = (q^+, \psi^+) + 2\langle g, \psi^+ \rangle_{L^2_-}. \tag{5}$$

Testing (1) with an odd test function $\psi^- \in \mathbb{W}^-$, we obtain that

$$(\mu \partial_z \phi^+, \psi^-) + (\sigma_t \phi^-, \psi^-) = (q^-, \psi^-),$$

which implies that $\phi^- = \frac{1}{\sigma_t}(q^- - \mu \partial_z \phi^+) \in \mathbb{W}^-$. Using this expression for ϕ^- in (5), we deduce that $u = \phi^+$ is a solution to the following problem; cf. [7].

Problem 3.1. Let $q \in L^2(\mathcal{D})$ and $g \in L^2_-$. Find $u \in \mathbb{W}^+$ such that

$$a(u, v) = \ell(v) \quad \text{for all } v \in \mathbb{W}^+. \tag{6}$$

where the bilinear form $a : \mathbb{W}^+ \times \mathbb{W}^+ \rightarrow \mathbb{R}$ is given by

$$a(u, v) = 2\langle u, v \rangle_{L^2_-} + \left(\frac{1}{\sigma_t} \mu \partial_z u, \mu \partial_z v\right) + ((\sigma_t - \sigma_s \mathcal{P})u, v), \tag{7}$$

and the linear form $\ell : \mathbb{W}^+ \rightarrow \mathbb{R}$ is defined as

$$\ell(v) = (q^+, v) + 2\langle g, \psi^+ \rangle_{L^2_-} + (q^-, \frac{1}{\sigma_t} \mu \partial_z v). \tag{8}$$

3.2. Well-posedness

We endow \mathbb{W}^+ with the norm induced by the bilinear form a defined in (7), i.e.,

$$\|u\|_{\mathbb{W}} = \|u\|_a = a(u, u)^{\frac{1}{2}} \quad \text{for } u \in \mathbb{W}^+. \tag{9}$$

Using the Cauchy–Schwarz inequality, we obtain the following result.

Lemma 3.2. The linear form $\ell : \mathbb{W} \rightarrow \mathbb{R}$ defined in (8) is bounded, i.e., for all $v \in \mathbb{W}^+$ it holds

$$\ell(v) \leq (\|q^+\|_{\frac{1}{\sigma_a}}^2 + \|q^-\|_{\frac{1}{\sigma_t}}^2 + 2\|g\|_{L^2_-}^2)^{\frac{1}{2}} \|v\|_a.$$

Since the space \mathbb{W}^+ endowed with the inner product induced by a is a Hilbert space, the unique solvability of Problem 3.1 is a direct consequence of the Riesz representation theorem.

Theorem 3.3. Let Assumption (A1) hold true. Then Problem 3.1 has a unique solution $u \in \mathbb{W}^+$. Moreover, we have the bound

$$\|u\|_a \leq (\|q^+\|_{\frac{1}{\sigma_a}}^2 + \|q^-\|_{\frac{1}{\sigma_t}}^2 + 2\|g\|_{L^2_-}^2)^{\frac{1}{2}}.$$

Remark 3.4. Setting $\phi^+ = u$ and $\phi^- = \frac{1}{\sigma_t}(q^- - \mu \partial_z u)$, one can show that $\mu \partial_z \phi^- \in L^2(\mathcal{D})$, i.e., $\phi = \phi^+ + \phi^- \in H^1_2(\mathcal{D})$ satisfies (1) in $L^2(\mathcal{D})$, cf. [7]. Using the trace Lemma 2.1 and partial-integration (3), we further can show that ϕ satisfies the boundary conditions (2) in the sense of traces. Hence, Theorem 3.3, independently, leads to a well-posedness result as Lemma 2.2 for (1)–(2).

3.3. DSA preconditioned source iteration in second order form

As a preparation for the numerical solution of the discrete systems that will be described below, let us discuss an iterative scheme in infinite dimensions for solving the radiative transfer equation. The basic idea is a standard one and consists of decoupling scattering and transport in order to compute successive approximation, viz., the source

iteration [19,20]. Next to the basic iteration, we describe a preconditioner which resembles diffusion synthetic acceleration (DSA) schemes using the notation of [20] or a KP_1 scheme using the terminology of [19].

In order to formulate the method, we introduce the following bilinear forms

$$k(u, v) = (\sigma_s \mathcal{P}u, v) \text{ and } b(u, v) = a(u, v) + k(u, v) \text{ for } u, v \in \mathbb{W}^+,$$

and denote the induced semi-norm and norm by $\|u\|_k$ and $\|u\|_b$, respectively.

The iteration scheme is defined as follows: For $u^k \in \mathbb{W}^+$ given, compute $u^{k+\frac{1}{2}} \in \mathbb{W}^+$ as the unique solution to

$$b(u^{k+\frac{1}{2}}, v) = k(u^k, v) + \ell(v) \text{ for all } v \in \mathbb{W}^+. \tag{10}$$

The half-step error $e^{k+\frac{1}{2}} = u - u^{k+\frac{1}{2}}$ satisfies

$$a(e^{k+\frac{1}{2}}, v) = k(u^{k+\frac{1}{2}} - u^k, v) \text{ for all } v \in \mathbb{W}^+. \tag{11}$$

The key idea is then to construct an easy-to-compute approximation to $e^{k+\frac{1}{2}}$ by Galerkin projection onto a suitable subspace $\mathbb{W}_1^+ \subset \mathbb{W}^+$. This approximation is then used to correct $u^{k+\frac{1}{2}}$ to obtain a more accurate approximation u^{k+1} to u . Define the following closed subspace of \mathbb{W}^+

$$\mathbb{W}_1^+ = \{u \in \mathbb{W}^+ : u = \mathcal{P}u\}, \tag{12}$$

i.e., \mathbb{W}_1^+ consists of functions in \mathbb{W}^+ that do not depend on μ . The correction $u_D^{k+\frac{1}{2}} \in \mathbb{W}_1^+$ is then computed by Galerkin projection of (11) to \mathbb{W}_1^+ :

$$a(u_D^{k+\frac{1}{2}}, v) = k(u^{k+\frac{1}{2}} - u^k, v) \text{ for all } v \in \mathbb{W}_1^+, \tag{13}$$

and the new iterate is defined as

$$u^{k+1} = u^{k+\frac{1}{2}} + u_D^{k+\frac{1}{2}}. \tag{14}$$

If $u_D^{k+\frac{1}{2}}$ is a good approximation to $e^{k+\frac{1}{2}}$, then $e^{k+1} = e^{k+\frac{1}{2}} - u_D^{k+\frac{1}{2}}$ is small. The convergence proof for the iteration $\mathbb{W}^+ \rightarrow \mathbb{W}^+$, $u^k \mapsto u^{k+1}$ is based on spectral analysis [31,32].

Lemma 3.5. *The half-step error $e^{k+\frac{1}{2}} = u - u^{k+\frac{1}{2}}$ of the iteration (10) satisfies*

$$\|e^{k+\frac{1}{2}}\|_a \leq c \|e^k\|_a,$$

with constant $c = \|\sigma_s/\sigma_t\|_\infty$.

Proof. We endow \mathbb{W}^+ with the inner product induced by the bilinear b in this proof, and define bounded, self-adjoint and positive operators A and K on \mathbb{W}^+ by

$$b(Au, v) = a(u, v), \quad b(Ku, v) = k(u, v) \text{ for } u, v \in \mathbb{W}^+.$$

Using $a = b - k$, we obtain that $A = I - K$. Using $u^{k+\frac{1}{2}} - u^k = e^k - e^{k+\frac{1}{2}}$, (11) can be written as

$$e^{k+\frac{1}{2}} = Ke^k.$$

We thus have that

$$\|e^{k+\frac{1}{2}}\|_a^2 = b((I - K)Ke^k, Ke^k) = b(K^2(I - K)^{\frac{1}{2}}e^k, (I - K)^{\frac{1}{2}}e^k) \leq \max \sigma(K)^2 \|(I - K)^{\frac{1}{2}}e^k\|_b^2 \leq c^2 \|e^k\|_a^2.$$

In the last step we have used the following bounds on the numerical range

$$0 \leq b(Kv, v) = k(v, v) \leq \left\| \frac{\sigma_s}{\sigma_t} \right\|_\infty (\sigma_t v, v) \leq c b(v, v),$$

which yields the spectral bounds $\sigma(K) \subset [0, c]$. \square

Theorem 3.6. *Let Assumption (A1) hold, and let $c = \|\sigma_s/\sigma_t\|_\infty < 1$ be as in Lemma 3.5. For any $u^0 \in \mathbb{W}^+$, the iteration defined by (10), (13), (14) converges linearly to the solution u of Problem 3.1 with*

$$\|u - u^{k+1}\|_a \leq c \|u - u^k\|_a.$$

Proof. Since $u_D^{k+\frac{1}{2}}$ is the orthogonal projection of $e^{k+\frac{1}{2}}$ to \mathbb{W}_1^+ in the a -inner product it holds that

$$\|e^{k+1}\|_a = \|e^{k+\frac{1}{2}} - u_D^{k+\frac{1}{2}}\|_a = \inf_{v \in \mathbb{W}_1^+} \|e^{k+\frac{1}{2}} - v\|_a \leq \|e^{k+\frac{1}{2}}\|_a.$$

The assertion then follows from Lemma 3.5. \square

Remark 3.7. The convergence analysis presented in this section carries over verbatim to multi-dimensional problems without symmetries, and it can be extended immediately to more general (symmetric and positive) scattering operators. Moreover, if a Poincaré–Friedrichs inequality is available, cf., e.g., [6], then the case $\sigma_a \geq 0$ can be treated similarly as long as σ_t is uniformly bounded away from 0, and the source iteration converges also in this situation.

Remark 3.8. Problem (13) is the weak formulation of the diffusion equation

$$-\partial_z(\frac{1}{3\sigma_t}\partial_z u_D) + \sigma_a u_D = f \quad \text{in } (0, Z),$$

with $f = \sigma_s \mathcal{P}(u^{k+\frac{1}{2}} - u^k)$, complemented by Robin boundary conditions, which shows the close relationship to DSA schemes.

Remark 3.9. The convergence analysis for the iteration without preconditioning, can alternatively be based on the following estimates. These estimates are the only ones in this paper that exploit that the scattering operator is related to the L^2 -projector \mathcal{P} . First note that

$$\|e^{k+\frac{1}{2}}\|_b^2 = \|\mathcal{P}e^{k+\frac{1}{2}}\|_{\sigma_t}^2 + \|(I - \mathcal{P})e^{k+\frac{1}{2}}\|_{\sigma_t}^2 + \|e^{k+\frac{1}{2}}\|_{L^2_-}^2 + \|\mu\partial_z e^{k+\frac{1}{2}}\|_{\frac{1}{\sigma_t}}^2$$

and that $\|e^{k+\frac{1}{2}}\|_b^2 = k(e^k, e^{k+\frac{1}{2}})$. Setting $c = \|\sigma_s/\sigma_t\|_\infty$, the Cauchy–Schwarz inequality yields

$$(1 - \frac{\varepsilon}{2})\|\mathcal{P}e^{k+\frac{1}{2}}\|_{\sigma_t}^2 + \|(I - \mathcal{P})e^{k+\frac{1}{2}}\|_{\sigma_t}^2 + \|e^{k+\frac{1}{2}}\|_{L^2_-}^2 + \|\mu\partial_z e^{k+\frac{1}{2}}\|_{\frac{1}{\sigma_t}}^2 \leq \frac{c^2}{2\varepsilon}\|\mathcal{P}e^k\|_{\sigma_t}^2$$

for any $\varepsilon \in (0, 2]$. Choosing $\varepsilon = 2$ shows that parts of the error are smoothed independently of c , i.e.,

$$\|(I - \mathcal{P})e^{k+\frac{1}{2}}\|_{\sigma_t}^2 + \|e^{k+\frac{1}{2}}\|_{L^2_-}^2 + \|\mu\partial_z e^{k+\frac{1}{2}}\|_{\frac{1}{\sigma_t}}^2 \leq \frac{c^2}{4}\|\mathcal{P}e^k\|_{\sigma_t}^2,$$

while the angular average is hardly damped. In any case, this shows that $\mathcal{P}e^k$ converges to zero. It remains open how to exploit such an estimate to improve the analysis of the DSA preconditioned scheme above as it seems difficult to relate the latter smoothing property to the best approximation error of $e^{k+\frac{1}{2}}$ in the a -norm.

4. Galerkin approximations

In this section, we construct conforming approximation spaces $\mathbb{W}_{h,N}^+ \subset \mathbb{W}^+$ in a two-step procedure. In a first step, we discretize the μ -variable using discontinuous ansatz functions. In a second step, we discretize the z -variable by continuous finite elements. Before stating the particular approximation space, we provide some general results. Let us begin with the definition of the discrete problem.

Problem 4.1. Let $q \in L^2(\mathcal{D})$, $g \in L^2_-$, $\mathbb{W}_{h,N}^+ \subset \mathbb{W}^+$ and let a and ℓ be defined as in Problem 3.1. Find $u_h \in \mathbb{W}_{h,N}^+$ such that for all $v \in \mathbb{W}_{h,N}^+$ there holds

$$a(u_h, v_h) = \ell(v_h).$$

Since the bilinear form a induces the energy norm that we use in our analysis, we immediately obtain the following best approximation result.

Theorem 4.2. Let $\mathbb{W}_{h,N}^+$ be a closed subspace of \mathbb{W}^+ . Then, there exists a unique solution $u_h \in \mathbb{W}_{h,N}^+$ of Problem 4.1 that satisfies the a-priori estimate

$$\|u_h\|_a \leq (\|q^+\|_{\frac{1}{\sigma_a}}^2 + \|q^-\|_{\frac{1}{\sigma_t}}^2 + 2\|g\|_{L^2_-}^2)^{\frac{1}{2}}, \tag{15}$$

and the following best approximation error estimate

$$\|u - u_h\|_a = \inf_{v_h \in \mathbb{W}_{h,N}^+} \|u - v_h\|_a. \tag{16}$$

In the next sections, we discuss some particular discretizations. We note that these generalize the spherical harmonics approach presented in [7].

4.1. hp-type semidiscretization in μ

Since we consider even functions, we require that the partition of the interval $[-1, 1]$ for the μ variable respects the point symmetry $\mu \mapsto -\mu$. For simplicity, we thus partition the interval $[0, 1]$ only, and the partition of $[-1, 0]$ is implicitly defined by reflection.

Let $N \in \mathbb{N}$ be a positive integer, and define intervals $\bar{\mu}_n = (\mu_{n-\frac{1}{2}}, \mu_{n+\frac{1}{2}})$, $n = 1, \dots, N$, such that $\mu_{\frac{1}{2}} = 0$ and $\mu_{N+\frac{1}{2}} = 1$, and set $\Delta\mu_n = \mu_{n+\frac{1}{2}} - \mu_{n-\frac{1}{2}}$ and $\mu_n = (\mu_{n+\frac{1}{2}} + \mu_{n-\frac{1}{2}})/2$. Denote $\chi_n(\mu)$ the characteristic function of the interval $\bar{\mu}_n$. For $\mu > 0$, we define the piecewise functions

$$Q_{n,l}(\mu) = \sqrt{\frac{2l+1}{2}} P_l\left(2 \frac{\mu - \mu_{n-\frac{1}{2}}}{\Delta\mu_n} - 1\right) \chi_n(\mu), \quad \mu > 0,$$

where P_l denotes the l th Legendre polynomial. Hence, $\{Q_{n,l}\}_{l=0}^L$ is an L^2 -orthonormal basis for the space of polynomials of degree L on each interval $\bar{\mu}_n$. For $\mu > 0$, we set $Q_{n,l}^\pm(\mu) = Q_{n,l}(\mu)$, and for $\mu < 0$, we set $Q_{n,l}^\pm(\mu) = \pm Q_{n,l}^\pm(-\mu)$. The semidiscretization of the even parts is then

$$u(z, \mu) \approx u_h(z, \mu) = \sum_{n=1}^N \sum_{l=0}^L \phi_{n,l}^+(z) Q_{n,l}^+(\mu).$$

Remark 4.3. If we partition the interval $[-1, 1]$ for the angular variable by a single element, we obtain truncated spherical harmonics approximations, see, e.g., [4,7]. Partitioning of $[-1, 1]$ into two symmetric intervals $\{(-1, 0), (0, 1)\}$ corresponds to the double P_L -method [4], which generalizes in multiple dimensions to half space moment methods [9]. The latter can resolve the non-smoothness of ϕ at $\mu = 0$, and, thus might yield spectral convergence on the intervals $\mu > 0$ and $\mu < 0$.

4.2. Fully discrete scheme

In order to obtain a conforming discretization, we approximate the coefficient functions $\phi_{n,l}^+$ using $H^1(0, Z)$ -conforming elements. Let $J \in \mathbb{N}$, and $\bar{z}_j = (z_{j-1}, z_j)$ be such that

$$[0, Z] = \cup_{j=1}^J \text{clos}(\bar{z}_j)$$

is a partition of $(0, Z)$. Let $p \geq 1$ and denote \mathbb{P}_p the space of polynomials of degree p . The full approximation space is then defined by

$$\mathbb{W}_{h,N}^+ = \{\psi_h^+(z, \mu) = \sum_{n=1}^N \sum_{l=0}^L \psi_{n,l}^+(z) Q_{n,l}^+(\mu) : \psi_{n,l}^+(z) \in H^1(0, Z), \psi_{n,l}^+ \in \mathbb{P}_p\}. \tag{17}$$

The choice (17) for the approximation space $\mathbb{W}_{h,N}^+$ corresponds to a hp -type finite element method, for which the assertion of Theorem 4.2 holds true.

Remark 4.4. If the solution $u_h \in \mathbb{W}_{h,N}^+$ to Problem 4.1 is computed, we compute even and odd approximations to the solution ϕ of (1) via $\phi_h^+ = u_h$ and the odd part $\phi_h^- \in \mathbb{W}_h^-$ as the solution to the variational problem $(\phi_h^-, \psi_h^-) = (\frac{1}{\sigma_t}(q^- - \mu \partial_z u_h), \psi_h^-)$ for all $\psi_h^- \in \mathbb{W}_h^-$, where

$$\mathbb{W}_{h,N}^- = \{\psi_h^-(z, \mu) = \sum_{n=1}^N \sum_{l=0}^{L+1} \psi_{n,l}^-(z) Q_{n,l}^-(\mu) : \psi_{n,l}^- \in \mathbb{P}_{p-1}\}.$$

We note that this space satisfies the compatibility condition $\mu \partial_z \mathbb{W}_{h,N}^+ \subset \mathbb{W}_{h,N}^-$, which makes this pair of approximation spaces suitable for a direct approximation of a corresponding mixed formulation, cf. [7]. The even-parity formulation that we consider here corresponds then to the Schur complement of the mixed problem, cf. [7]. The reader should note the different degrees in the polynomial approximations, e.g., if ϕ_h^+ is piecewise constant in angle, then ϕ_h^- is piecewise linear.

5. Discrete preconditioned source iteration

In order to solve the discrete variational problem defined in Problem 4.1, we proceed as in Section 3.3 but with \mathbb{W}^+ and \mathbb{W}_1^+ replaced by $\mathbb{W}_{h,N}^+$ and $\mathbb{W}_{h,1}^+$, respectively. We note that $\mathbb{W}_{h,1}^+ \subset \mathbb{W}_1^+$ consists of functions in $\mathbb{W}_{h,N}^+$ that do not depend on μ .

The finite dimensional counterpart of the DSA preconditioned source iteration is then defined as follows: For given $u_h^k \in \mathbb{W}_{h,N}^+$, compute $u_h^{k+\frac{1}{2}} \in \mathbb{W}_{h,N}^+$ as the unique solution to

$$b(u_h^{k+\frac{1}{2}}, v_h) = k(u_h^k, v_h) + \ell(v_h) \quad \text{for all } v_h \in \mathbb{W}_{h,N}^+. \tag{18}$$

The correction $u_{h,D}^{k+\frac{1}{2}} \in \mathbb{W}_{h,1}^+$ is defined by Galerkin projection of $e_h^{k+\frac{1}{2}}$ to $\mathbb{W}_{h,1}^+$:

$$a(u_{h,D}^{k+\frac{1}{2}}, v_h) = k(u_h^{k+\frac{1}{2}} - u_h^k, v_h) \quad \text{for all } v_h \in \mathbb{W}_{h,1}^+, \tag{19}$$

and the new iterate is defined as

$$u_h^{k+1} = u_h^{k+\frac{1}{2}} + u_{h,D}^{k+\frac{1}{2}}. \tag{20}$$

Using the same arguments as above, we obtain the following convergence result.

Theorem 5.1. *Let Assumption (A1) hold, and let $c < 1$ be as in Lemma 3.5. For any $u_h^0 \in \mathbb{W}_{h,N}^+$, the iteration defined by (18), (19), (20) converges linearly with*

$$\|u_h - u_h^{k+1}\|_a \leq c \|u_h - u_h^k\|_a.$$

Remark 5.2. Similar to Remark 3.8, $u_{h,D}^{k+\frac{1}{2}}$ is the Galerkin projection to $\mathbb{W}_{h,1}^+$ of the weak solution to

$$-\partial_z(D(z)\partial_z u_D) + \sigma_a u_D = f, \quad 0 < z < Z,$$

with μ -grid dependent diffusion coefficient $D(z)$ and $f = \sigma_s \mathcal{P}(u_h^{k+\frac{1}{2}} - u_h^k)$. If piecewise constant functions in angle are employed, then $D(z) = \frac{1}{3\sigma_t(z)}(1 + \frac{1}{4} \sum_{n=1}^N \Delta\mu_n^3)$.

Remark 5.3. Once the scattering term in the right-hand side of (18) has been computed, the half-step iterate $u_h^{k+\frac{1}{2}}$ can be computed independently for each direction, and, thus, its computation can be parallelized.

6. Numerical examples

In this section, we report on the accuracy of the proposed discretization scheme and its efficient numerical solution using the DSA preconditioned source iteration of Section 5. We restrict our discussion to a low-order method that offers local resolution. To do so, we fix $p = 1$ and $L = 0$ in the definition of $\mathbb{W}_{h,N}^+$, while N might be large. Hence, the approximation space $\mathbb{W}_{h,N}^+$ consists of discontinuous, piecewise constant functions in the angular variable and continuous, piecewise linear functions in z .

6.1. Manufactured solutions

To investigate the convergence behavior, we use manufactured solutions, i.e., the exact solution is

$$\phi(z, \mu) = |\mu|e^{-\mu}e^{-z(1-z)}, \tag{21}$$

with parameters $\sigma_a = 1/100$, $\sigma_s(z) = 2 + \sin(\pi z)/2$ and $Z = 1$, and source terms defined accordingly. We computed the numerical solution u_h using the DSA preconditioned iteration (18), (19), (20). We stopped the iteration using the a-posteriori stopping rule

$$\|u_h^k - u_h^{k-1}\|_a \leq \varepsilon,$$

where $\varepsilon = 10^{-10}$ is a chosen tolerance. The approximations of the even and odd parts of the solutions are recovered as described in Remark 4.4.

For the chosen parameters, the predicted convergence rate is $c \approx 0.996$. Table 1 shows the errors for different discretization parameters N and J . As expected we observe a linear rate of convergence with respect to N , cf. Theorem 4.2. In addition, we observe that the preconditioned source iteration converged within at most 15 iterations, and the expression $\|u_h^k - u_h^{k-1}\|_a$ decreased by 0.21 in each iteration. The convergence rate with respect to J is initially quadratic, which is better than predicted by Theorem 4.2, and then saturates for fixed $N = 8192$. As before, the preconditioned source iteration converged within at most 15 iterations with a decrease by a factor of 0.21 of $\|u_h^k - u_h^{k-1}\|_a$.

The observed convergence rate is thus as the one obtained by classical Fourier analysis for constant coefficients and periodic boundary conditions, which is bounded by 0.2247 [20]. Furthermore, we observe that the rate of convergence does not depend on the grid size as predicted by Theorem 5.1, cf. Remark 5.2, i.e., using the terminology of [20], our discrete diffusion approximation is consistently discretized.

In the next section, we present a more detailed study of spectrum of the preconditioned operator.

6.2. Eigenvalue studies of the preconditioned operator

In this section, we consider the spectrum of the error propagation operator $\mathcal{P}e_h^n \mapsto \mathcal{P}e_h^{n+1}$, where \mathcal{P} is the L^2 -projection onto constants in angle defined in Section 2 and e_h^n is the sequence of errors generated by the DSA preconditioned source iteration, cf. Remark 3.9. The function $\mathcal{P}e_h^n$ depends only on z , and, assuming $\sigma_s > 0$, we can measure the projected error using the norm induced by σ_s , i.e.,

$$\|\mathcal{P}e_h^n\|_{\sigma_s} = \|e_h^n\|_k.$$

Table 1

Observed errors $E_h = \|\phi - \phi_h\|_{L^2(\mathcal{D})}$ between finite element solution ϕ_h and the manufactured solution ϕ defined in (21) together with the rate of convergence of E_h . Left: Convergence for different discretization parameters N , and $J = 256$. Right: Convergence for different discretization parameters J and $N = 8192$.

N	E_h	Rate	J	E_h	Rate
512	1.61e-04		16	7.88e-04	
1024	8.07e-05	0.99	32	1.99e-04	1.98
2048	4.04e-05	0.99	64	5.14e-05	1.96
4096	2.04e-05	0.99	128	1.63e-05	1.66
8192	1.06e-05	0.95	256	1.06e-05	0.62

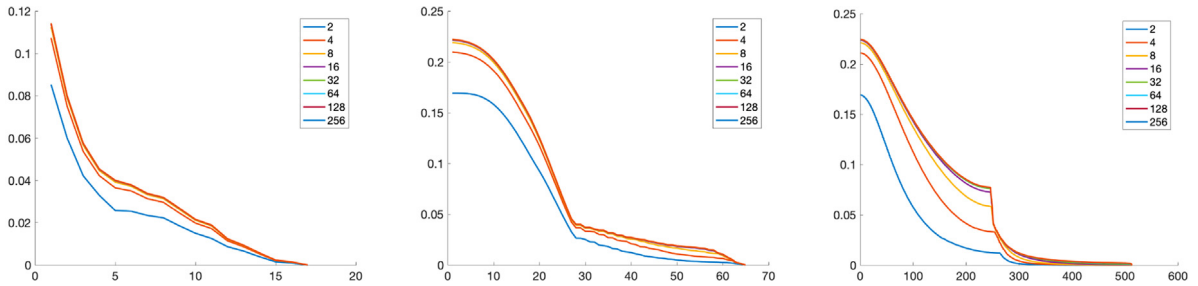


Fig. 1. Spectra of the error propagation operator $\mathcal{P}e_h^n \mapsto \mathcal{P}e_h^{n+1}$ for different spatial discretizations $J = 16, 64, 512$ (from left to right). Each plot contains the corresponding spectra for $N = 2^i, i = 1, \dots, 8$.

We choose the following scattering and absorption parameters

$$\sigma_s(z) = \begin{cases} 2 + \sin(2\pi z), & z \leq \frac{1}{2} \\ 102 + \sin(2\pi z), & z > \frac{1}{2}, \end{cases} \quad \sigma_a(z) = \begin{cases} 10.01, & z \leq \frac{1}{2} \\ 0.01, & z > \frac{1}{2}. \end{cases}$$

We notice that both parameters have huge jumps and that the predicted convergence rate is $c = \|\sigma_s/\sigma_t\|_\infty \approx 0.9999$, cf. Theorem 3.6.

In Fig. 1 we plot the spectrum of the error propagation operator for different mesh sizes. All eigenvalues are bounded from above by 0.2247, which is inline with the results of [19,20]. For each spatial discretization, we observe that the corresponding eigenvalues are monotonically increasing with N . The spectra for $N \geq 16$ lie on top of each other, indicating convergence of the eigenvalues. In particular, also for the coarse grid approximations the spectrum is uniformly bounded by 0.2247, again confirming the robustness of the method with respect to different approximations.

6.3. Multi-dimensional problems

Although the theory has been presented for slab problems, it becomes clear from our proofs that the results carry over verbatim to truly multi-dimensional problems, for which the radiative transfer equation writes as

$$s \cdot \nabla_x \phi(x, s) + \sigma_t(x)\phi(x, s) = \sigma_s(x)(\mathcal{P}\phi)(x, s) + q(x, s).$$

In the following, let us consider homogeneous inflow boundary conditions, and homogeneity of the problem with respect to one spatial variable, i.e., we assume that the solution depends only on $x \in \mathcal{R} \subset \mathbb{R}^2$ and $s \in \mathbb{S}^2 \subset \mathbb{R}^3$.

We discretize $L^2(\mathbb{S}^2)$ by approximating \mathbb{S}^2 using a geodesic polyhedron consisting of flat triangles, see Fig. 2. The approximation space in angle then consists of standard discontinuous finite element spaces associated to this triangulation. In the following, we focus on piecewise constant approximations, but higher order approximations are straightforward if the geometry approximation is also of higher order. The next paragraph is concerned with the accuracy of our method.

Manufactured solutions. Let $\mathcal{R} = (0, 1) \times (0, 1)$ be the unit square, and let $\sigma_s = 2$ and $\sigma_a = 0.01$. Define the source function q such that

$$\phi(x, s) = \sin(\pi x_1) \sin(\pi x_2) (1 + s_1 + s_2^2 + s_3^3) \tag{22}$$

is the exact solution. In Table 2 we report on the numerical errors for different computational grids.

As expected from our error estimates, we observe linear convergence of the error in terms of the mesh size until saturation occurs. Note that for $N = 4096$ and $J = 4225$ the number of degrees of freedom is 17 305 600. The proven contraction rate for the iteration is $c = 0.995$, while the observed maximal value of $\|u_h^k - u_h^{k-1}\|_a / \|u_h^{k-1} - u_h^{k-2}\|_a$, i.e., the minimal reduction rate, was 0.2 indicating much faster convergence of the iteration. After at most 16 iterations the stopping criterion $\|u_h^k - u_h^{k-1}\|_a \leq \varepsilon$ was reached.

Table 2

Observed errors $E_h = \|\phi^+ - \phi_h^+\|_\alpha$ between finite element solution ϕ_h and the manufactured solution ϕ defined in (22) together with the rate of convergence of E_h . Left: Convergence for different discretization parameters N , and $J = 4225$ vertices. Right: Convergence for different discretization parameters J and $N = 4096$ triangles on a half-sphere.

N	E_h	Rate	J	E_h	Rate
4	6.55e-01		25	6.89e-01	
16	3.48e-01	0.91	81	4.12e-01	0.75
64	1.87e-01	0.90	289	2.25e-01	0.87
256	1.06e-01	0.81	1089	1.18e-01	0.93
1024	7.37e-02	0.53	4225	6.30e-02	0.91

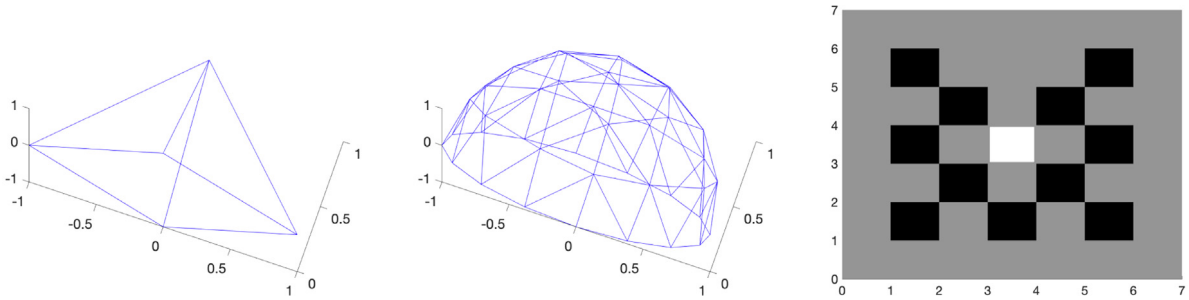


Fig. 2. Left and middle: Approximation of the half-sphere with $N = 4$ and $N = 64$ triangles. Right: Geometry of the lattice problem.

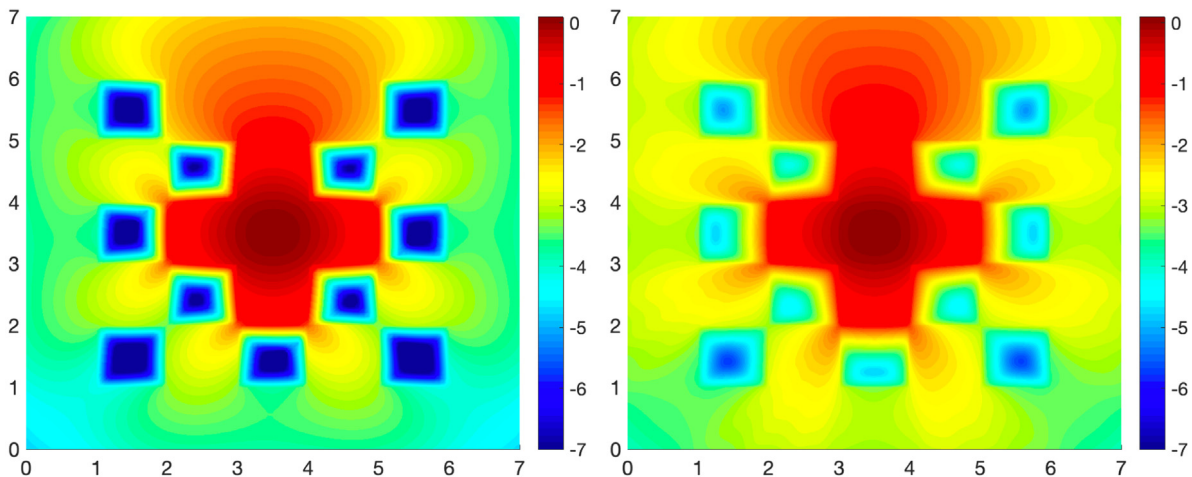


Fig. 3. Angular average of the computed solution in a \log_{10} -scale for the lattice problem for $J = 9801$ spatial vertices and $N = 4$ triangles on a half-sphere (left) and $J = 78961$ spatial vertices and $N = 64$ triangles on a half-sphere (right).

The lattice problem. A non-smooth test case without analytical solution is the lattice problem [27], which models the core of a neutron reactor. The computational domain is a square $\mathcal{R} = (0, 7) \times (0, 7)$. The absorption and scattering rates are piecewise constant functions. We define $\sigma_a = 10$ in the black regions shown in Fig. 2, and $\sigma_a = 0$ elsewhere. We set $\sigma_s = 1$ in the gray and white regions and $\sigma_s = 0$ elsewhere. The source is defined by $q(x, s) = 1$ in the white region and $q(x, s) = 0$ elsewhere. Note that due to the availability of a Poincaré–Friedrichs inequality [6], the case $\sigma_a = 0$ leads to a well-posed radiative transfer problem, and, since $\sigma_s + \sigma_a \geq 1$, the theory presented here is applicable. Moreover, the constant c will depend on the constant from the Poincaré–Friedrichs inequality and $c < 1$.

In Fig. 3 we show the angular averages of the computed solutions for two different grids with $J = 9801$ vertices in the spatial grid and $N = 4$ triangles on a half-sphere and for $J = 78961$ and $N = 64$, respectively. We note that our solutions do not suffer from ray effects, cf. [4,27]. The preconditioned source iteration converged with 9 and 17 iterations for the coarse grid approximation and for the fine grid approximation, respectively. This amounts to an error reduction per iteration of at least 0.04 for the coarse grid discretization and of at least 0.2 for the fine grid discretization.

Table 3

Iteration counts k and minimal reduction rates for $\|u_h^k - u_h^{k-1}\|_a$ for the lattice problem with scaled parameters σ_s^δ , σ_a^δ and q^δ for different δ and discretizations with N triangles on a half-sphere and J vertices in the spatial mesh.

$1/\delta$	$J = 9801$				$J = 78961$			
	$N = 4$		$N = 64$		$N = 4$		$N = 64$	
	k	Rate	k	Rate	k	Rate	k	Rate
1	9	0.04	15	0.16	9	0.04	15	0.17
10	9	0.06	15	0.22	9	0.06	16	0.25
100	8	0.06	13	0.22	9	0.07	15	0.27
1000	5	0.01	7	0.06	6	0.05	10	0.17

Diffusion scaling. Next, let us investigate the behavior of the preconditioned source iteration for scaled parameters. Introducing a scale parameter $\delta > 0$, a diffusion limit is obtained by the scaling [33]

$$\frac{\bar{\sigma}_s(x)}{\delta}, \quad \delta \bar{\sigma}_a(x), \quad \delta \bar{q}(x),$$

when both parameters $\bar{\sigma}_s$ and $\bar{\sigma}_a$ are bounded and strictly bounded away from zero. Since this is not the case for the lattice problem, we consider the following parameters

$$\sigma_s^\delta(x) = \frac{\sigma_s(x) + 1/10}{\delta}, \quad \sigma_a^\delta = \delta(\sigma_a(x) + 1/10), \quad q^\delta(x, s) = \delta q(x).$$

For $\delta \rightarrow 0$, the corresponding solution u^δ will converge to the solution of a diffusion problem; for non-smooth coefficients see [24]. The parameter c defined in Lemma 3.5 satisfies $c \approx 1 - \delta^2$. Table 3 shows the iteration counts and the minimum reduction of $\|u_h^k - u_h^{k-1}\|_a$ during the iteration. We observe that the preconditioned iteration is robust with respect to $\delta \rightarrow 0$ for different meshes. The convergence rate on the finest grid is, however, slightly worse than the convergence rate for slab problems.

7. Conclusions

We investigated discontinuous angular and continuous spatial approximations of the even-parity formulation for the radiative transfer equation. Certain instances of these approximations are closely related to classical discretizations, such as truncated spherical harmonics approximations, double P_N -methods or discrete ordinates methods.

We considered a diffusion accelerated preconditioned source iteration for the solution of the resulting variational problems that has been formulated in infinite dimensions. Convergence rates of this iteration have been proven. The Galerkin approach used for the discretization allowed to translate the results for the infinite dimensional iteration directly to the discrete problems. In particular, the discrete iteration converges independently of the chosen resolution.

The theoretically proven convergence rate in Theorem 3.6 is not robust in the limit of large scattering, while numerical results show that in practice the preconditioned iteration converges robustly even in scattering dominated problems. One approach to obtain an improved convergence rates estimate is to estimate the best approximation error $\inf_{v \in \mathbb{W}_1^+} \|e^{k+\frac{1}{2}} - v\|_a$, which, however, seems rather difficult, and we postpone a corresponding rigorous analysis to future research.

The term diffusion acceleration is linked to the usage of the space \mathbb{W}_1^+ in (12) that consists of functions constant in angle. This choice is, however, not essential, and other closed subspace can be employed, which allows for the construction of multi-level schemes, cf. also [16,34–36]. The multi-level approach might lead to a feasible approach to estimate the best approximation error.

In any case, the DSA preconditioner can be combined with a conjugate gradient method in order to further reduce the number of iterations. Moreover, unlike many discrete ordinates schemes, the numerical approximation did not suffer from the ray effect in our numerical examples. We postpone a detailed study of this phenomenon to future research.

CRedit authorship contribution statement

Olena Paliı: Methodology, Software, Formal analysis, Investigation, Writing - review & editing, Visualization. **Matthias Schlottbom:** Conceptualization, Methodology, Software, Formal analysis, Investigation, Writing - original draft, Writing - review & editing, Visualization, Project administration, Supervision.

Acknowledgments

The authors would like to thank Herbert Egger and Markus Bachmayr for stimulating discussions.

References

- [1] S. Chandrasekhar, Radiative Transfer, Dover Publications, Inc., 1960.
- [2] K.M. Case, P.F. Zweifel, Linear Transport Theory, Addison-Wesley, Reading, 1967.
- [3] V.S. Vladimirov, Mathematical Problems in the One-Velocity Theory of Particle Transport, Tech. rep., Atomic Energy of Canada Ltd. AECL-1661, 1961, translated from Transactions of the V.A. Steklov Mathematical Institute (61).
- [4] E.E. Lewis, W.F. Miller Jr., Computational Methods of Neutron Transport, John Wiley & Sons, Inc., New York Chichester Brisbane Toronto Singapore, 1984.
- [5] J. Pitkäranta, Approximate solution of the transport equation by methods of Galerkin type, J. Math. Anal. Appl. 60 (1977) 186–210.
- [6] T.A. Manteuffel, K.J. Ressel, G. Starke, A boundary functional for the least-squares finite-element solution for neutron transport problems, SIAM J. Numer. Anal. 2 (2000) 556–586.
- [7] H. Egger, M. Schlottbom, A mixed variational framework for the radiative transfer equation, Math. Models Methods Appl. Sci. 22 (2012) 1150014.
- [8] H. Egger, M. Schlottbom, A perfectly matched layer approach for radiative transfer in highly scattering regimes., SIAM J. Numer. Anal. 57 (5) (2019) 2166–2188.
- [9] B. Dubroca, M. Frank, A. Klar, G. Thömmes, A half space moment approximation to the radiative heat transfer equations, ZAMM Z. Angew. Math. Mech. 83 (12) (2003) 853–858, <http://dx.doi.org/10.1002/zamm.200310055>.
- [10] M. Frank, Approximate models for radiative transfer, Bull. Inst. Math. Acad. Sin. (N.S.) 2 (2) (2007) 409–432.
- [11] C. Johnson, J. Pitkäranta, Convergence of a fully discrete scheme for two-dimensional neutron transport, SIAM J. Numer. Anal. 20 (1983) 951–966.
- [12] M. Asadzadeh, Analysis of a fully discrete scheme for neutron transport in two-dimensional geometry, SIAM J. Numer. Anal. 23 (1986) 543–561.
- [13] W.H. Reed, T.R. Hill, Triangular Mesh Methods for the Neutron Transport Equation, Tech. rep., Los Alamos Scientific Laboratory of the University of California, 1973.
- [14] T. Wareing, J. McGhee, J. Morel, S. Pautz, Discontinuous finite element S_N methods on three-dimensional unstructured grids, Nucl. Sci. Eng. 138 (2001) 1–13.
- [15] J.C. Ragusa, J.-L. Guermond, G. Kanschat, A robust S_N -DG-approximation for radiation transport in optically thick and diffusive regimes, J. Comput. Phys. 231 (4) (2012) 1947–1962, <http://dx.doi.org/10.1016/j.jcp.2011.11.017>.
- [16] G. Kanschat, J.-C. Ragusa, A robust multigrid preconditioner for S_N DG approximation of monochromatic, isotropic radiation transport problems, SIAM J. Sci. Comput. 36 (5) (2014) A2326–A2345, <http://dx.doi.org/10.1137/13091600X>.
- [17] J. Kópházi, D. Lathouwers, A space-angle DGfEM approach for the Boltzmann radiation transport equation with local angular refinement, J. Comput. Phys. 297 (2015) 637–668, <http://dx.doi.org/10.1016/j.jcp.2015.05.031>.
- [18] P. Clarke, H. Wang, J. Garrard, R. Abedi, S. Mudaliar, Space-angle discontinuous Galerkin method for plane-parallel radiative transfer equation, J. Quant. Spectrosc. Radiat. Transfer 233 (2019) 87–98, <http://dx.doi.org/10.1016/j.jqsrt.2019.02.027>.
- [19] G.I. Marchuk, V.I. Lebedev, Numerical Methods in the Theory of Neutron Transport, Harwood Academic Publishers, Chur, London, Paris, New York, 1986.
- [20] M.L. Adams, E.W. Larsen, Fast iterative methods for discrete-ordinates particle transport calculations, Prog. Nucl. Energy 40 (1) (2002) 3–159.
- [21] W. Dahmen, F. Gruber, O. Mula, An adaptive nested source term iteration for radiative transfer equations, Math. Comp. (2019) 1, <http://dx.doi.org/10.1090/mcom/3505>.
- [22] J.S. Warsa, T.A. Wareing, J.E. Morel, Krylov iterative methods and the degraded effectiveness of diffusion synthetic acceleration for multidimensional S_N calculations in problems with material discontinuities, Nucl. Sci. Eng. 147 (3) (2004) 218–248, <http://dx.doi.org/10.13182/NSE02-14>.
- [23] E.W. Larsen, J.B. Keller, Asymptotic solution of neutron transport problems for small mean free paths, J. Math. Phys. 15 (1974) 75–81, <http://dx.doi.org/10.1063/1.1666510>.
- [24] H. Egger, M. Schlottbom, Diffusion asymptotics for linear transport with low regularity, Asymptot. Anal. 89 (3–4) (2014) 365–377.
- [25] K. Ren, R. Zhang, Y. Zhong, A fast algorithm for radiative transport in isotropic media, J. Comput. Phys. 399 (2019) 108958, <http://dx.doi.org/10.1016/j.jcp.2019.108958>.
- [26] Y. Fan, J. An, L. Ying, Fast algorithms for integral formulations of steady-state radiative transfer equation, J. Comput. Phys. 380 (2019) 191–211, <http://dx.doi.org/10.1016/j.jcp.2018.12.014>.
- [27] T.A. Brunner, Forms of approximate radiation transport, in: Nuclear Mathematical and Computational Sciences: A Century in Review, A Century Anew Gatlinburg, American Nuclear Society, LaGrange Park, IL, 2003, Tennessee, April 6–11, 2003.
- [28] V. Agoshkov, Boundary Value Problems for Transport Equations, Modeling and Simulation in Science, Engineering and Technology, Birkhäuser, Boston, 1998.
- [29] H. Egger, M. Schlottbom, An L^p theory for stationary radiative transfer, Appl. Anal. 93 (6) (2014) 1283–1296, <http://dx.doi.org/10.1080/00036811.2013.826798>.
- [30] J.C. Blake, Domain Decomposition Methods for Nuclear Reactor Modelling with Diffusion Acceleration (Ph.D. thesis), University of Bath, 2016.
- [31] G. Helmborg, Introduction to spectral theory in Hilbert space, North-Holland Series in Applied Mathematics and Mechanics, vol. 6, North-Holland Publishing Co., Amsterdam-London: Wiley Interscience Division John Wiley & Sons, Inc., New York, 1969, p. xiii+346.
- [32] D. Werner, Funktionalanalysis, extended ed., Springer-Verlag, Berlin, 2000, p. xii+501.
- [33] R. Dautray, J.L. Lions, Mathematical Analysis and Numerical Methods for Science and Technology, Evolution Problems II, Vol. 6, Springer, Berlin, 1993.
- [34] J.E. Morel, T.A. Manteuffel, An angular multigrid acceleration technique for S_N equations with highly forward-peaked scattering, Nucl. Sci. Eng. 107 (4) (1991) 330–342, <http://dx.doi.org/10.13182/nse91-a23795>.
- [35] B. Lee, A multigrid framework for S_N discretizations of the Boltzmann transport equation, SIAM J. Sci. Comput. 34 (4) (2012) A2018–A2047, <http://dx.doi.org/10.1137/110841199>.
- [36] J.D. Densmore, D.F. Gill, J.M. Pounders, Cellwise block iteration as a multigrid smoother for discrete-ordinates radiation-transport calculations, J. Comput. Theoret. Transp. 46 (1) (2016) 20–45, <http://dx.doi.org/10.1080/23324309.2016.1161650>.